A New Func-Pso Controller For Optimal Conversion Of Noise Pollution Into Electricity

Kriti[1], Arunesh Kumar Singh[2], Shahida Khatoon[3]
[1,2,3]Department of Electrical Engineering, Jamia Millia Islamia, New Delhi-110025, India

Abstract: This paper presents the development of a new controller for the optimal conversion of noise pollution into electricity. The process of converting the noise pollution to electricity is quite challenging because more noise, uncontrolled pressure, and more voltage deviation have been obtained. In order to overcome such issues, an objective function has been developed by considering all constraint parameters like noise, pressure, and voltage. Further, the objective function has been controlled by particle swarm optimization (PSO). By doing this, the proposed method has been given the name FUNC-PSO controller. It is observed that the least noise, least voltage deviation, and optimal sound pressure have been attained with the proposed FUNC-PSO controller in comparison to the existing controller for the smooth conversion of noise pollution to electricity. The overall work has been validated on the experimental setup.
Keywords: noise, voltage, pressure, FUNC-PSO, controller

I. INTRODUCTION

Noise pollution is one of the most common and significant types of environmental pollution. Unwanted sound energy refers to noise pollution. It is an excessive or disturbing sound that causes discomfort and interferes with normal activities. It is a low-frequency sound-pressure signal that is underutilized, although it has the potential to generate electrical energy.

Electricity requirements are increasing rapidly, and renewable and alternative sources of electricity production are a necessity of the hour. Nowadays, scientists and researchers are delving into finding alternate energy resources and techniques for energy harvesting[1]. Noise pollution energy harvesting is a process that utilizes the acoustic nature of noise pollution to generate electrical signals. The noise pollution energy harvester converts the noise pollution into usable electrical energy. Noise pollution energy harvesters can help the electricity grid to fulfill the increasing electricity requirement, and can also be used to run low-power appliances [2].

Noise pollution can be broadly classified into the following categories:
- Transportation noise pollution
- Industrial noise pollution
- Community noise pollution

Transportation noise pollution can be further divided on the basis of the type of transport as Road-traffic noise pollution, Railway noise pollution, Airport noise pollution, and Marine noise pollution.

Industrial noise pollution is caused due to heavy industries, factories, and construction sites.

Community noise pollution may occur because of large gatherings such as shopping centers, stadiums, discos, etc. Among the various categories, road traffic noise is the highest type and constitutes approximately fifty percent of total noise pollution[3].

The acoustic signal is a low-frequency sound pressure signal that can be captured by some conventional transducers such as piezoelectric transducers and electromagnetic transducers. Since the noise acoustic signal has relatively low energy, the sensor to captures the noise pollution signal must have high energy density. The thin-film piezoelectric sensor called PVDF (Polyvinylidene Fluoride) polymer sensor and electret microphone can be used to convert noise pollution into electric signals. In recent years, triboelectric nanogenerators (TENGs), sensors, and acoustic metamaterials have been used for acoustic energy harvesting[4].

This research work is divided into two parts: developing the noise pollution electric energy conversion system (NPECS) and optimizing the NPECS response.

II. LITERATURE REVIEW

The sound-electric energy conversion is a classical process that came into existence with the invention of the telephone in the late 18th century. With the development of technology, the sound-electric and electric-sound conversion process has been simplified and more efficient[5]. The sound is a mechanical vibration that travels in the atmosphere. The process of harvesting sound energy is called acoustic energy harvesting. Acoustic energy harvesting (AEH) is a process to captures the sound energy and uses it for low-level power generation. In 2013, a low-frequency AEH model was developed for low-power generation. The sound level of 100dB at 199 Hz is used to generate the 0.498 mW power and 1.51V electric output [6]. The Helmholtz resonator was used for energy harvesting with a multilayer PVDF film sensor for low-power generation. A sound pressure of 15Pa at 850 Hz frequency was utilized to develop 0.19 microwatts [7]. The Helmholtz resonator provides resonance conditions to the sound pressure signal in the resonator. When the frequency of the sound matches the frequency of the resonator, the signal gets amplified, and a large output can be produced. The roadside traffic noise-based energy harvester was introduced in 2017. The 75dB SPL level produces 0.78 volts per hour and is used for supercapacitor charging [8]. A PVDF film was fabricated using graphene and metal electrodes for energy harvesting (EH) in 2017 [9]. In the year 2021, the triboelectric nano-generator is used to develop 1.5V output from the 90-decibel sound pressure at 140 Hz frequency [10]. A multi-frequency sound EH system was developed to convert 200 dB into a 5.31- 8.66nW output [11] . The noise generated from the district cooling plant, where the chiller generates a continuous noise of 96 dB is utilized for energy harvesting. The above system generated a notable 25.8 mV output voltage [12]. The recent researches suggest implementing the wearable and flexible devices made of nanomaterials such as zinc oxide (ZnO). These devices can convert ambient energies such as solar, sound, and motion to supply the implantable and remotely located devices. The concept of hybrid nanogenerators using photoelectric, piezoelectric, and triboelectric energy harvesting can be utilized [13].

I.SOUND-ELECTRIC CONVERSION MECHANISM

The sound propagation can be expressed as follows:

$$\frac{\partial^2 p}{\partial x^2} - \frac{1}{c^2}\frac{\partial^2 p}{\partial t^2} = 0 \qquad (1)$$

Here, p is the sound pressure, x is the position, and t is the time.   The relation between sound speed, wavelength, and frequency is given by,

$$c = \lambda f \qquad (2)$$

Where c is the speed of sound, λ is the wavelength, f is the frequency of sound [14].
The equivalent sound pressure level (SPL) is the measure of noise pollution and is expressed as follows:

$$SPL = 20\log\left(\frac{p}{p_{\text{ref}}}\right) \qquad (3)$$

Here, p_{ref} is the reference sound pressure.
In air, $p_{\text{ref}} = 20\mu Pa$
The expression for sound's pressure is given as follows:

$$p = p_{\text{ref}}10^{\left(\frac{\text{SPL}}{20}\right)} \qquad (4)$$

The frequency of the sound can be matched with the resonant frequency of the resonator to obtain the maximum result. At resonance condition,

$$f = f_H \qquad (5)$$

The frequency of the resonator can be determined using the shape and dimensions of the resonator. The resonator is a chamber or collection unit. The entrance of the chamber is called as neck of the resonator. The neck diameter should be less than the height of the resonator [15].

$$f_H = \frac{c}{2\pi}\sqrt{\frac{A}{V_R L_R}} \qquad (6)$$

Here, V_R is the static volume of the neck, L_R is the equivalent length of the neck, A is the area of neck, and c is the speed of sound.

The sound-electric converter plays an important role in converting sound into electric signal. There are various transducers such electrostatic sensors, electromagnetic sensors, piezoelectric sensors, etc. that can be utilized for sound-electric conversion mechanism. The sound pressure signal vibrates surface of the sound-electric converter and generates the electrical signal [16].

The output voltage of the electrostatic sensor is,

$$V_{ES} = V_{Bias}\frac{pA}{kx_0} \qquad (7)$$

Here, V_{Bias} is the DC bias voltage, A is the diaphragm area, x_0 is the initial gap, k is the spring constant.

The output voltage of the electromagnetic sensor is,

$$V_{EM} = \frac{NBlp}{z} \qquad (8)$$

Here, N is the number of turns of the coil, l is the effective length of the wire, B is the magnetic flux density, z is the acoustic impedance.

Due to higher flexibility and greater volume density, piezoelectric sensors are mostly used as sound-electric converter. In response to the pressure (p), the output voltage of the piezo sensor is expressed as,

The output voltage of the electromagnetic sensor is,

$$V_{PZ} = \frac{dpAt}{\varepsilon} \qquad (9)$$

Here, d is charge coefficient, A is the surface area, t is the thickness of the sensor, ε is the permittivity of the piezoelectric material.

The sound is a low frequency pressure signal that can only develop a low-level electric signal. The developed electrical signal must be gone through proper amplification and rectification process to increase the utility of the sound-electric conversion mechanism.

PROTOTYPE MODEL DEVELOPMENT
The block diagram of the NPECS is shown in Figure 1. In this circuit, the input noise is applied to the combination of the piezoelectric transducer (PVDF sensor) and electromagnetic transducer (microphone). A glass chamber is used to provide isolation and collect the input noise signal. The electrical output signal is observed using the multimeter and used to glow the LED. The sound pressure level of the input noise pollution can be observed using the SPL meter.
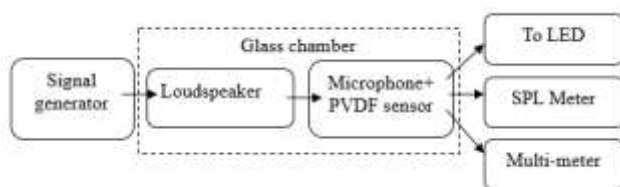

Fig.1 Block diagram of NPECS

The signal generator generates the sinusoidal signal given as,

$$V(t) = V_0 \sin \omega t \tag{10}$$

The loudspeaker is acting as a sound or noise pollution source. Figure 2 shows the structure of the loudspeaker and Figure 3 shows the electrical equivalent of the loudspeaker.

The cone's displacement (x) due to the loudspeaker's voltage is,

$$x(t) = x_0 \sin \omega t \tag{11}$$

Here, x_0 is the initial distance, ω is the frequency (in radians), and t is the time.

The velocity and the acceleration of the cone are the derivation of the cone's displacement and are given as,

$$v = \frac{dx}{dt} = \omega x_0 \cos\omega t \tag{12}$$

$$a = \frac{dv}{dt} = -\omega^2 x_0 \sin\omega t \tag{13}$$
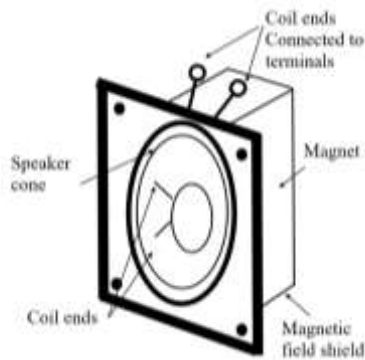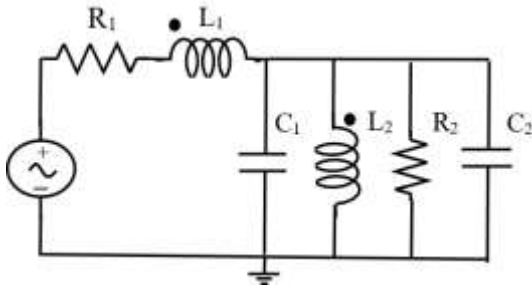

Fig.2 Loudspeaker structure

Fig.3 Electrical equivalent of the Loudspeaker

The sound pressure generated by the loudspeaker depends upon the acceleration (a), density (ρ), cone's surface area (S), and radius of the cone (r) as follows:

$$p = \frac{\rho S}{2\pi r} a \tag{14}$$

The above expression can be modified as,

$$p = -\frac{\rho S}{2\pi r} \omega^2 x \tag{15}$$

Hence, the relation between the sound pressure and the voltage is given as,

$$p = \frac{\rho S}{2\pi r} \frac{V_0 BL}{R_{LM} M_{LM}} \sin \omega t \tag{16}$$

Here, BL is the force factor. M_{LM} is the moving mass, R_{LM} is the DC resistance of the purely resistive loudspeaker [17].

The piezoelectric sensors can be used to convert the sound pressure into electric charge. When the sound pressure (p) is applied to the piezoelectric transducer, it vibrates the sensor and create some electric charge across the opposite faces of the sensor. The fundamental equations for the piezoelectric transducer as given below.

$$D_i = e_{ij}S_j + \varepsilon S_{ii}E_i \qquad (17)$$

$$T_j = C_{ij}^E S_j - e_{ij}E_i \qquad (18)$$

Here, Tj can be stress in N/m², S_j is strain, E_i is electric field, Di is displacement, C_{ij}^E is elastic stiffness constant, εS_{ii} is permittivity at unit strain S. e is piezo-electric constant.
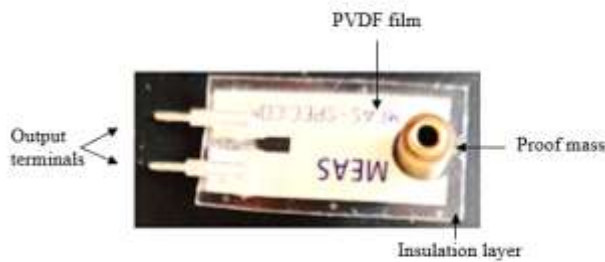

Fig.4 Commercially available piezoelectric sensor with proof mass

The piezoelectric sensor works in two modes: d_{31} and d_{33}. The direction of charge accumulation is perpendicular to the direction of applied pressure in d_{31} mode. In d_{33} mode, the charge accumulates in the same direction as of applied pressure.

Consider a piezo sensor exerts a force (F) on a cross-sectional area (A) under stress (δ) is given by

$$F = \delta A \qquad (19)$$

The induced electric charge (Q) is related to the electric field (E), area (A), and change in the piezoelectric sensor's length (ϵ) as follows:

$$Q = d_{31}EA\epsilon \qquad (20)$$

The current flowing through the piezo sensor is given as,

$$I = \frac{dQ}{dt} \qquad (21)$$

The voltage developed by the piezoelectric sensor is,

$$V = \frac{1}{C}\int \frac{dQ}{dt}dt = \frac{Q}{C} \qquad (22)$$

In a piezoelectric transducer, the charge collected on the piezoelectric surface is derived from the fundamental equations (17, 18) of the piezoelectric material as follows:

$$Q = b \int_0^{L_b}(d_{31}T + \varepsilon_{33}E)dx \qquad (23)$$

Here, T is the mechanical stress, E is electric filed, d_{31} piezoelectric constant, L_b is the upper limit of the piezoelectric base length, and b is constant.
Modify the above expression as follows:

$$Q = \frac{bt_s d_{31}}{2}[\phi(0) - \phi(L_b)] + bL_b \varepsilon_{33} E \quad (24)$$

Consider the slope of beam deflection is ϕ and, substrate thickness is t_{piezo}.
The electric field developed is,

$$E = -\frac{V}{t_{piezo}} \quad (25)$$

The final expression of the electric charge is,

$$Q = \frac{bt_s d_{31}}{2}[\phi(0) - \phi(L_b)] - bL_b \varepsilon_{33}\frac{V}{t_{piezo}} \quad (26)$$

The current (I) is related to frequency (ω), and resistance (R) as follows:

$$I = \omega Q = \frac{V}{R} \quad (27)$$

The magnitude of the current is given as follows:

$$I = \frac{\omega bt_s d_{31}[\phi(0) - \phi(L_b)]}{2\left(1 + bL_b \varepsilon_{33}\frac{\omega R}{t_p}\right)} \quad (28)$$

Here, t_s is the thickness of the piezolelctric subtrate, R is the load resistance, ε_{33} applied strain, ω is the angular frequency [18].
The microphone is used to convert the sound signal into electric signal based on the principle of the electromagnetic induction.
The voltage (V) is induced in a closed loop circuit is proportional to the rate of change in the magnetic flux (ϕ).

$$V = N\frac{d\phi}{dt} \quad (29)$$

In this circuit setup, a combination of electromagnetic sensor and piezoelectric sensors are used. Hence the theoretical expression for the output voltage is given as follows:

$$V = N\frac{d\phi}{dt} + \frac{Q}{C} \quad (30)$$

Substitute the value of charge (Q).

$$V = N\frac{d\phi}{dt} + \frac{Ed_{33}\varepsilon_{11}dA_d}{C} \quad (31)$$

Here, $N\frac{d\phi}{dt}$ is the voltage developed in the microphone, and $\frac{Ed_{33}\varepsilon_{11}dA_d}{C}$ is the output voltage of the piezo sensor [19].

II. Experimentation Work
In this section of the paper, the experimentation work of the NPECS is explained. A glass chamber as shown in figure 5 is used to confine the acoustic input signal. Multiple tests have been performed keeping the sound source in the open

environment, at some distance from chamber, and inside the chamber. The NPECS unit were place inside the chamber during the experimentation. While keeping the sound sensor outside at fixed distance from the chamber, the sound entrance is used for inletting the sound signal otherwise it is kept closed.
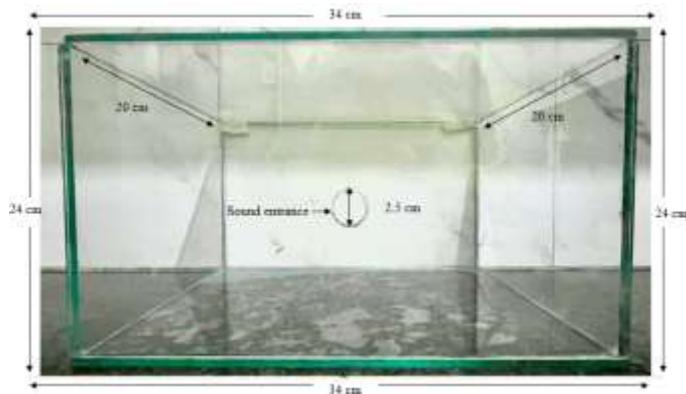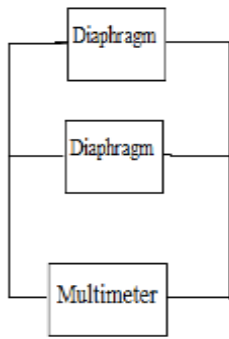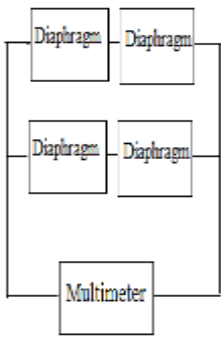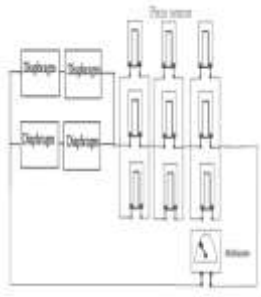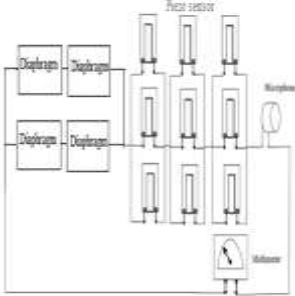

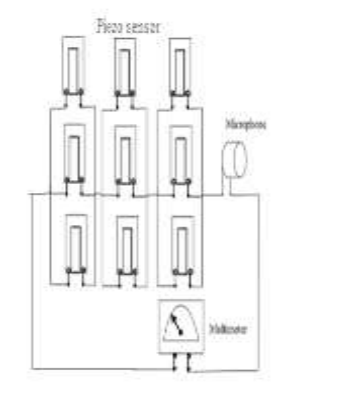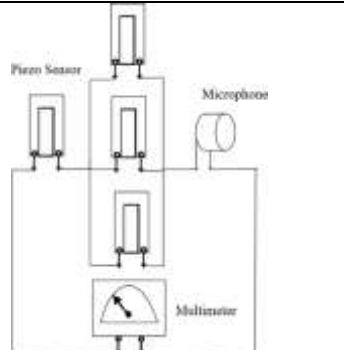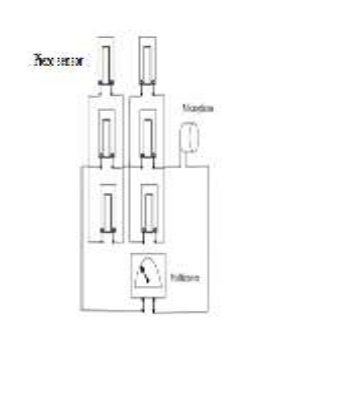Fig.5 Glass chamber used for experimentation

Various configurations of the sensor's connection are tested for the experiments. The conventional sensors such as loudspeaker, diaphragm, and modern sensors such as PVDF film piezoelectric sensor, electret microphone are connected in hybrid connections to develop the output voltage across and glow a low-voltage light emitting diode. The circuit response is depicted in table 1.

Table.1 Hardware model response

S. No.	Circuit arrangement	Open-circuit voltage	Load voltage (at 1000 Ω)	Circuit Diagram
1	1 Diaphragm	22 mV	0 V	
2	3 Diaphragms (in series)	22 mV	0 V	

	2 Diaphragms (in parallel)	34mV	0 V	
3	4 Diaphragms (2 in series+ 2 in parallel)	50mV	0 V	
4	4 Diaghragms+9 Piezo sensors (3x3 matrix)	25mV	0 V	
5	4 Diaghragms+9 Piezo sensors (3x3 matrix) + Microphone	1V	20 mV	

6	9 Piezo sensors (3x3 matrix) + Microphone	1.4V	36 mV	
7	4 Piezo sensors (1 series+3 parallel) + Microphone	3.7V	300 mV	
8	6 Piezo sensors (3 parallel+3 parallel) + Microphone	4.82V	434 mV	

The best-performed model is shown in row-8 of the table-1.
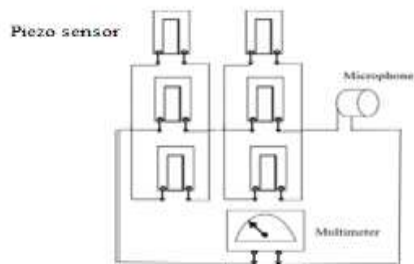

Fig.6 Circuit configuration of NPECS

An experimental setup of the NPECS is depicted in Figure 7. Two sets of the 3-parallel connected Piezo sensor are connected in series and an electret microphone is also connected in series with this combination. An android app 'sound meter' is used for SPL monitoring and the vehicular noise of range 80 dB-110 dB is recorded inside the glass chamber.

Fig.7 Experimental setup of NPECS

The following observations are observed from the experiment. The highest observed input sound signal is 110 decibels. Hence, the testing is performed at a constant input sound pressure level of 110 dB.

Table 2 - Observation table of the experiment

S. No.	Parameter	Maximum obtained value
1	Open-circuit output voltage	4820 mV
2	Output voltage with a connected LED	482 mV
3	Output voltage at 1000 Ohms load resistance	434 mV
4	Circuit current	0.434 mA
5	Output power	0.118 mW

III. Design Of Proposed Controller

To objective of the work is to optimize the output parameters of the noise pollution energy converter. The input parameters are sound pressure, SPL input, current and voltage generated by loudspeaker, frequency and the voltage developed from the piezoelectric sensor and electromagnetic sensor.

A) Formulation of objective function

An objective function can be framed by considering the above expressions as follows:

$$f(k_1, k_2, k_3, k_4, k_5, P, Vo) \quad\quad (32)$$
$$= k_1 20\log\left(\frac{p}{p_{ref}}\right) + k_2 \frac{\rho S}{2\pi r}\frac{V_0 BL}{R_{LM}M_{LM}}$$
$$+ k_3 \frac{\omega bt_s d_{31}[\phi(0) - \phi(L_b)]}{2\left(1 + bL_b\varepsilon_{33}\frac{\omega R}{t_{piezo}}\right)} + k_4\, N \times \frac{d\phi}{dt}$$
$$+ k_5 \frac{Ed_{33}\varepsilon_{11}dA_d}{C}$$

Now the objective function shown in Eq.32 will be trained by using PSO. In Eq.32, there are certain variables like k1,k2,k3,k4,k5 involved in the expression. These variables will be trained by using PSO which makes the controller as FUNC-PSO controller.

B) Training of objective function by PSO

One method of adaptive optimisation is the PSO technique. Its exceptional processing power makes it a preferred option for a wide range of technological applications. Because the PSO technique combines more gradually and swiftly than other approaches utilizing populations stochastic optimization, it offers a speedy means to determine the overall makeup of the system. Fig. 8 illustrates the flowchart that explains the PSO procedure. The following are the three primary stages of the PSO method.:

i) Assessing each particle's fit.

ii) Changing each particle's velocity and position to improve its global and local optimum fitness and ideal position.

iii) To optimize the PSO method, the flowchart gives data on the particle's position & velocity.

The general formula for the location as well as velocity particle in the following cycle is given by Equations 33 and 34.

$$v(t + 1) = \omega(t)v(t) + c_1 r_1 (pbest(t) - x(t)) + c_2 r_2 (gbest(t) - x(t)) \tag{33}$$

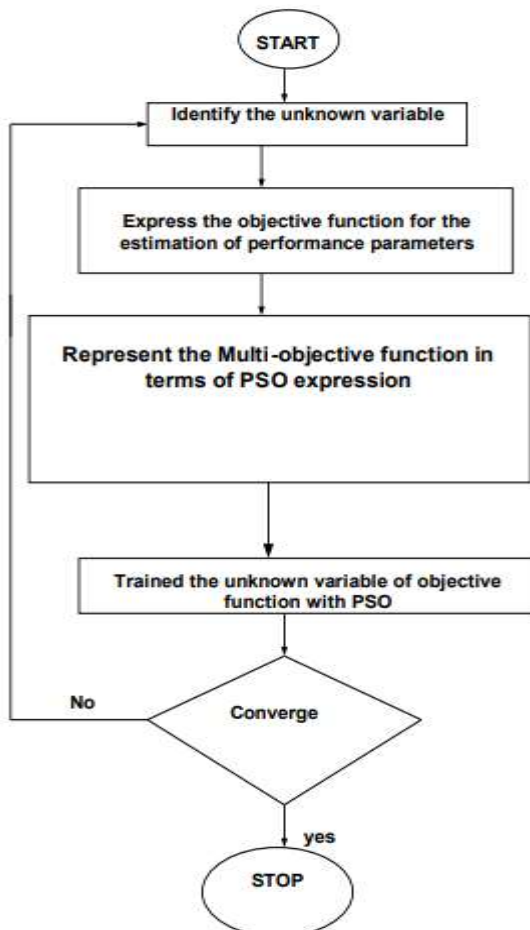$$x(t+1) = x(t) + v(t+1) \tag{34}$$

Fig.8 Flowchart explanation of the PSO

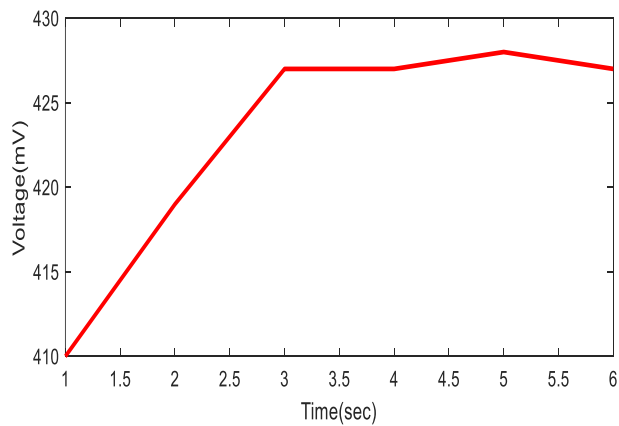## V. Performance parameters and analysis with proposed controller

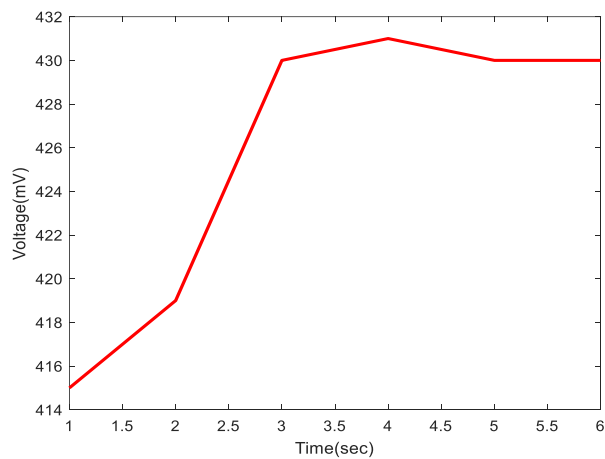Fig.9 Generated voltage variation at 15dB with proposed controller

Fig.10 Generated voltage variation at 16dB with proposed controller
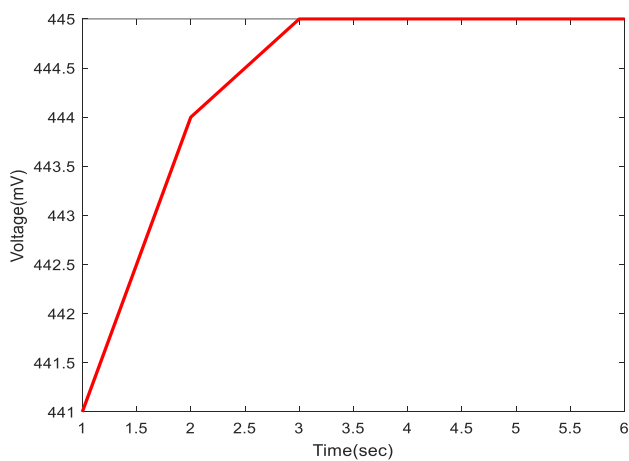

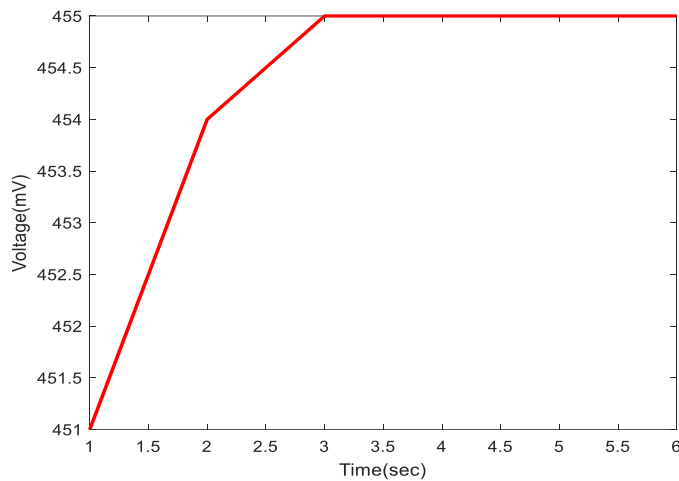Fig.11 Generated voltage variation at 18dB with proposed controller

Fig.12 Generated voltage variation at 20 dB with proposed controller

Table.3 Comparison of voltage deviation at different pressure level with proposed controller

Pressure (dB)	Voltage deviation(%) with proposed controller	Voltage deviation(%) with Ref.[3]	Voltage deviation(%) Ref.[17]
15	3.6	5.9	6.8
16	3.9	6.1	7.2
17	4.1	6.4	7.4
18	4.6	6.9	8.1
20	4.9	7.1	8.9

Table.4 Comparison of change in noise level at different pressure level with proposed controller

Pressure (dB)	Change in noise level (%) with proposed controller	Change in noise level (%) at Ref.[3]	Change in noise level (%) at Ref.[17]
15	4.1	5.9	7.2
16	4.6	6.1	7.4
17	5.1	7.5	8.7
18	6.2	8.9	9.1
20	6.5	8.7	9.4

The characteristics of generated voltages at different pressure level with proposed method are shown from Fig.9 to Fig.12. Further, comparison of voltage deviation (%) and change in noise level (%) for various pressure levels with proposed controller and existing methods (Ref.[3] and Ref. [17]) have been shown in Table.3 and Table.4. It is observed that least voltage deviation and least noise level have been attained with proposed controller in contrast to existing methods.

VI. CONCLUSION

The design and development of a novel controller for the best possible transformation of noise pollution into electrical power is presented in this work. Due to increased noise, uncontrolled pressure, and voltage fluctuation, the process of turning noise pollution into energy is quite difficult. An objective function has been created to address these problems

by taking into account all constraint parameters, such as noise, pressure, and voltage. Furthermore, particle swarm optimization (PSO) has been used to control the objective function. As a result, the suggested approach has been dubbed FUNC-PSO controller. Comparing the suggested FUNC-PSO controller to the current controller for the seamless conversion of noise pollution to electricity, it has been found that the former achieves the lowest noise, the lowest voltage variation, and the best sound pressure. The complete work has been performed and tested on experimental set up.

REFERENCES

[1]   M. Yuan, Z. Cao, J. Luo, and X. Chou, "Recent developments of acoustic energy harvesting: A review," Jan. 11, 2019, *MDPI AG*. doi: 10.3390/mi10010048.

[2]   J. Choi, I. Jung, and C. Y. Kang, "A brief review of sound energy harvesting," *Nano Energy*, vol. 56, pp. 169–183, Feb. 2019, doi: 10.1016/j.nanoen.2018.11.036.

[3]   W. Yang, J. He, C. He, and M. Cai, "Evaluation of urban traffic noise pollution based on noise maps," *Transp Res D Transp Environ*, vol. 87, p. 102516, 2020, doi: 10.1016/j.trd.2020.102516.

[4]   B. Mahanty, S. K. Ghosh, K. Maity, S. Roy, S. Sarkar, and D. Mandal, "All-fiber pyro- And piezo-electric nanogenerator for IoT based self-powered health-care monitoring," *Mater Adv*, vol. 2, no. 13, pp. 4370–4379, Jul. 2021, doi: 10.1039/d1ma00131k.

[5]   P. Malcovati and A. Baschirotto, "The evolution of integrated interfaces for MEMS microphones," *Micromachines (Basel)*, vol. 9, no. 7, Jun. 2018, doi: 10.3390/mi9070323.

[6]   B. Li, J. H. You, and Y. J. Kim, "Low frequency acoustic energy harvesting using PZT piezoelectric plates in a straight tube resonator," *Smart Mater Struct*, vol. 22, no. 5, 2013, doi: 10.1088/0964-1726/22/5/055013.

[7]   H. Y. Lee and B. Choi, "A multilayer PVDF composite cantilever in the Helmholtz resonator for energy harvesting from sound pressure," *Smart Mater Struct*, vol. 22, no. 11, Nov. 2013, doi: 10.1088/0964-1726/22/11/115025.

[8]   C. S. Salvador *et al.*, "Development of a traffic noise energy harvesting standalone system using piezoelectric transducers and super-capacitor," in *Proceedings - 25th International Conference on Systems Engineering, ICSEng 2017*, Institute of Electrical and Electronics Engineers Inc., Nov. 2017, pp. 370–376. doi: 10.1109/ICSEng.2017.77.

[9]   S. Park, Y. Kim, H. Jung, J. Y. Park, N. Lee, and Y. Seo, "Energy harvesting efficiency of piezoelectric polymer film with graphene and metal electrodes," *Sci Rep*, vol. 7, no. 1, Dec. 2017, doi: 10.1038/s41598-017-17791-3.

[10]   H. Yuan *et al.*, "A High-Performance Coniform Helmholtz Resonator-Based Triboelectric Nanogenerator for Acoustic Energy Harvesting," pp. 1–14, 2021.

[11]   C. Song *et al.*, "Multi-frequency sound energy harvesting using Helmholtz resonators with irradiated cross-linked polypropylene ferroelectret films," *AIP Adv*, vol. 11, no. 11, Nov. 2021, doi: 10.1063/5.0060305.

[12]   Z. Ismaili, M. A. Mustapha, M. O. Abdullah, G. Ismaili, and A. S. Mohamed Pauzan, "Converting industrial noise into useful electrical energy: a review and case study on acoustic energy harvesting in district cooling plants," *Sustainable Energy Research*, vol. 12, no. 1, p. 18, Apr. 2025, doi: 10.1186/s40807-025-00156-0.

[13]   K. Adaikalam and H.-S. Kim, "Hybrid Energy Harvesting Applications of ZnO Nanorods for Future Implantable and Wearable Devices," *Micromachines (Basel)*, vol. 16, no. 6, p. 605, May 2025, doi: 10.3390/mi16060605.

[14]   Frank. Fahy and David. Thompson, *Fundamentals of sound and vibration*. Zed Books, 2021.

[15]   R. Hedayati and S. P. Lakshmanan, "Active Acoustic Metamaterial Based on Helmholtz Resonators to Absorb Broadband Low-Frequency Noise," *Materials*, vol. 17, no. 4, Feb. 2024, doi: 10.3390/ma17040962.

[16]   Z. Lin *et al.*, "Insights into Materials, Physics, and Applications in Flexible and Wearable Acoustic Sensing Technology," Mar. 01, 2024, *John Wiley and Sons Inc*. doi: 10.1002/adma.202306880.

[17]   A. Zagubień and K. Wolniewicz, "Impact of measuring microphone location on the result of environmental noise assessment," *Applied Acoustics*, vol. 172, Jan. 2021, doi: 10.1016/j.apacoust.2020.107662.

[18]   A. K. Singh, S. Khatoon, and K. Tripathi, "DEVELOPMENT AND VALIDATION OF AN EFFICIENT NOISE POLLUTION ENERGY CONVERSION SYSTEM," *Journal of Dynamics and Control*, pp. 35–47, Jan. 2025, doi: 10.71058/jodac.v9i1005.

[19]   X. Shan, Z. Xu, R. Song, and T. Xie, "A new mathematical model for a piezoelectric-electromagnetic hybrid energy harvester," *Ferroelectrics*, vol. 450, no. 1, pp. 57–65, 2013, doi: 10.1080/00150193.2013.838490.